

## Mixing of Two Miscible Liquids in T-Shaped Microdevices

Gianni Orsi, Chiara Galletti, Elisabetta Brunazzi\*, Roberto Mauri

Dipartimento di Ingegneria Civile ed Industriale, Università di Pisa, Largo L. Lazzarino, 56126 Pisa, Italy  
 e.brunazzi@diccism.unipi.it

Numerical simulations were performed to study the flow fields and mixing characteristics of liquid flows converging in a T-shaped micromixer, when the two inlet fluids are both water or water and ethanol. We showed that at smaller Reynolds number,  $Re < 100$ , mixing is controlled by transverse diffusion, and therefore by the residence times of each fluids. Accordingly, mixing ethanol and water is slightly easier than mixing water with water, due to the fact that, as ethanol is slightly more viscous than water and therefore it is slower, the residence time of water-ethanol mixtures is larger than that of the water-water case. On the other hand, at larger Reynolds number, mixing water and ethanol may take considerably longer, as the onset of engulfment is retarded and occurs at larger Reynolds number, namely increasing from  $Re \cong 140$  in the water-water case to  $Re \cong 230$  in the water-ethanol case. This is due to the fact that a water-ethanol mixture has a viscosity that is up to almost three times larger than that of water; therefore, at the confluence of the T-mixer, the water and the ethanol streams are separated by a quite viscous layer of a water-ethanol mixture, that hampers any vortex formation, thus retarding mixing.

### 1. Introduction

Mixing two different fluids in a micromixer is one of the most basic processes in microfluidics. Due to the small size of the device, pressure driven flows in simple channels (i.e. with smooth walls) are laminar and mostly uniaxial, so that confluent liquids tend to flow side by side. On the other hand, as the Schmidt number (i.e. the ratio  $\nu/D$  between kinematic viscosity and molecular diffusivity) is typically very large, the Peclet number is large, that is  $Pe = U \cdot d/D$ , where  $U$  is the mean fluid velocity, and  $d$  the hydraulic diameter. Accordingly, in the absence of any transverse convection, complete mixing is reached after the distance  $L \cong d \cdot Pe$  along the channel that can be prohibitively long. The easiest way to overcome this difficulty and enhance mixing is to induce transverse flows through clever geometries (Hessel et al., 2005). The simplest one consists of a T-shaped micromixer. T-shaped micromixers have been investigated extensively in recent years, as they are quite suitable to carry out fundamental studies to understand mixing at the microscale (Nguyen and Wu, 2005). Most of the investigators have confined themselves to the mixing of two identical liquids, assuming that in one of them a dilute solute is dissolved. Such systems were studied by Engler et al. (2004) both numerically and experimentally, finding that at the confluence of the two streams three flow regimes may occur, depending on the Reynolds number, namely stratified laminar flow, vortex flow and engulfment flow. Also, as noted by Galletti et al. (2012), the morphology of the fluid flow at the confluence, and consequently the mixing efficiency as well, is strongly influenced by the inlet flow conditions. However, low investigation has been devoted to studying the mixing process between two different, albeit miscible, fluids from a fundamental perspective, despite two-fluid mixing being an essential process in many microfluidic devices. For example, various pharmaceutical, chemical, biomedical and biochemical processes involve the mixing of two fluids, including nano-drugs preparation by anti-solvent methods, DNA purification, polymerase chain reaction (PCR), enzyme reaction, and protein folding, whose performance relies on the effective and rapid mixing of samples and reagents (Vural-Gursel et al., 2012). So, for example, in the works by Chung and Shih (2008), Ansari et al. (2010), and Lin et al. (2011), where W-E mixtures were considered, the main objective was determining the best geometrical set up to optimize mixing. The present study focuses on the comparison between the case where the two inlet fluids are both water (W-W case) and that when they consist of water and ethanol (W-E case), using a

simple T-type passive micro-mixer with Reynolds numbers ranging from 1 to 300. In order to do that, a commercial Computational Fluid Dynamics (CFD) code, Fluent 13 by Ansys Inc., was used to solve the three-dimensional equations of motion for a non-ideal W-E mixture that takes the non-ideality of the W-E mixture into account. In fact, the influence of the mixture non-ideality, above all its strong increase in viscosity, has not been accounted for in all previous works.

## 2. Simulation technique

### 2.1 Governing equations

Consider two fluids converging into a T-junction. The two inlet streams have the same temperature, so that, as the heat of mixing has a negligible effect here, we may assume that the process is isothermal. In general, the governing equations at steady state are:

$$\nabla \cdot (\rho \mathbf{u}) = 0, \quad (1)$$

$$\rho \mathbf{u} \cdot \nabla \mathbf{u} + \nabla p = \nabla \cdot \left[ \mu (\nabla \mathbf{u} + \nabla \mathbf{u}^T) \right] + \rho \mathbf{g}, \quad (2)$$

$$\rho \mathbf{u} \cdot \nabla \phi = \nabla \cdot (\rho D \nabla \phi). \quad (3)$$

Here,  $\mathbf{u}$  denotes the velocity vector,  $\rho$  the fluid density,  $p$  the pressure,  $\mu$  the viscosity,  $\mathbf{g}$  the gravity acceleration,  $D$  the molecular diffusivity and  $\phi$  the mass fraction of one of the two inlet fluids, say fluid A. If the two fluids are identical, we can imagine adding a very small amount of contaminant, i.e. a dye, to one of the fluids (which therefore continue to have the same physical properties) and therefore  $\phi$  indicates the (normalized) dye mass fraction. These equations have been solved with boundary conditions consisting of no-slip velocity and no-mass-flux at the channel walls, with a constant ambient pressure at the exit. In addition, at the entrance a given flow profile was imposed, assuming fully developed fluid conditions. In this way, we avoid the undesired complications connected to the inlet fluid conditions, that we have analyzed in a separated work (Galletti et al., 2012). The fully developed velocity profile in a closed rectangular conduit can be easily obtained by solving the Navier-Stokes equations with no-slip boundary conditions at the walls and a constant axial pressure gradient (Happel and Brenner, 1973). The most delicate part of this simulation concerns the dependence of viscosity,  $\mu$ , and density,  $\rho$ , of the W-E mixture on the mixture composition,  $\phi$ . In fact, while the default setting of the Fluent CFD code consists of a linear dependence of both  $\rho$  and  $\mu$  on  $\phi$ , we know that the matter is quite different. For example, as density is the inverse of the specific volume, we know that, in general:

$$\frac{1}{\rho} = \frac{\phi}{\rho_A} + \frac{1-\phi}{\rho_B} + \Delta v_{mix}(\phi), \quad (4)$$

where  $\rho_A$  and  $\rho_B$  are the densities of pure fluids A and B, respectively, while  $\Delta v_{mix}(\phi)$  is the volume of mixing, that is the volume, per unit mass, that the mixture gains (or loses) upon mixing the two components with a given mass fraction  $\phi$ . When  $\Delta v_{mix} = 0$ , as for example in regular mixtures, volumes are conserved. That, however, does not apply to a W-E mixture, as it is well known that upon mixing 1 liter of water with 1 liter of ethanol, the volume of the resulting mixture is 1.9 liter, corresponding to a 5% loss of volume (Perry and Green, 1997). Regarding viscosity, being it the resistance of a fluid against the diffusive transport of momentum, it is known (Kern, 1965) that for an ideal mixture, we have:  $\mu^{-1} = \phi \mu_A^{-1} + (1-\phi) \mu_B^{-1}$ , where  $\mu_A$  and  $\mu_B$  are the viscosities of pure fluids A and B. Therefore, we can write:

$$\frac{1}{\mu} = \frac{\phi}{\mu_A} + \frac{1-\phi}{\mu_B} + \Delta f_{mix}(\phi), \quad (5)$$

where  $\Delta f_{mix}(\phi)$  is a fluidity of mixing, taking into account the non-ideality of the mixture. This term is particularly important in our case, as it is well known that at 20°C a mixture of ethanol and water with  $0.3 < \phi < 0.6$  has a viscosity which is almost three times that of pure water. Similar behaviour is observed for many aqueous mixtures of organic solvents (see Dizechi and Marschall, 1982). The values of density and viscosity of the pure fluids were set equal to  $\rho_A = 998 \text{ kg m}^{-3}$  and  $\mu_A = 10^{-3} \text{ kg m}^{-1} \text{ s}^{-1}$  for water (fluid A) and  $\rho_B = 789 \text{ kg m}^{-3}$  and  $\mu_B = 1.2 \times 10^{-3} \text{ kg m}^{-1} \text{ s}^{-1}$  for ethanol (fluid B), respectively, which correspond to their respective values at a 20°C temperature. In addition, the density and the viscosity of the W-E mixture were evaluated through Eqs. (4) and (5), where the volume of mixing and the fluidity of mixing are fitted from the

experimental measurements by Dizechi and Marschall (1982), obtaining the curves shown in Figure 1. It is worth noting that the default setting of the Fluent CFD code, i.e. a linear dependence of both  $\rho$  and  $\mu$  on  $\phi$ , appears to work reasonably well for  $\rho$  (this is obviously a casual coincidence), while it is completely wrong for  $\mu$ .

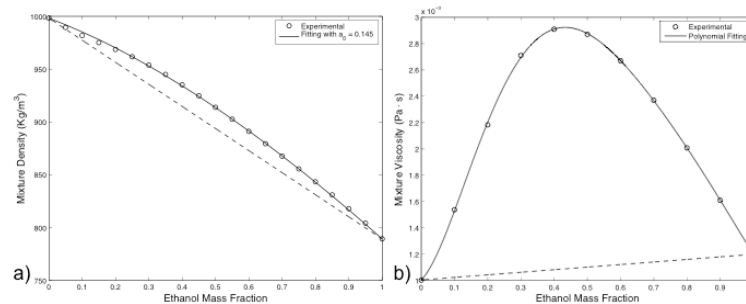


Figure 1: a) Density vs. ethanol mass fraction; b) viscosity vs. ethanol mass fraction. Dotted lines show the mixture density and viscosity when a linear dependence on mass fraction is assumed.

## 2.2 Geometry and numerical model

The geometric setting of our simulation consists of a T-shaped micro-device, where the mixing channel has a rectangular cross section with a 2:1 aspect ratio, with length  $L = 5H$ , while the inlet channels are identical, with square cross section and length  $L' = L = 5H$ . In particular, the dimensions indicated in all our figures are referred to the particular case with  $H = 100 \mu\text{m}$ , as this corresponds to the geometric setup used numerically by Bothe et al. (2008) and experimentally by Hoffmann et al. (2006). The grid consists of cubic elements with  $H/34$  edge, leading to a mesh of  $34 \times 68$  elements in each cross section of the mixing channel, thus in agreement with the recommendation by Hussong et al. (2009), regarding how to accurately describe the velocity fields. A second order discretization scheme was used to solve all the governing equations. Simulations were typically considered converging when the normalized residuals for velocities were stationary with iterations and fell below  $1 \times 10^{-6}$ , although smaller residuals were required in specific cases, especially near the engulfment (Galletti et al., 2012). In addition, a grid independence study was performed on the velocity field, showing that, repeating the numerical simulation with smaller cubical elements (i.e. with  $H/64$  edge), the simulations performed at maximum flow rate,  $Re = 300$ , give results (in particular, the degree of mixing) that do not differ from the original simulation. Similar analysis was also conducted by Roudgar et al. (2012), using a slightly different geometric setup.

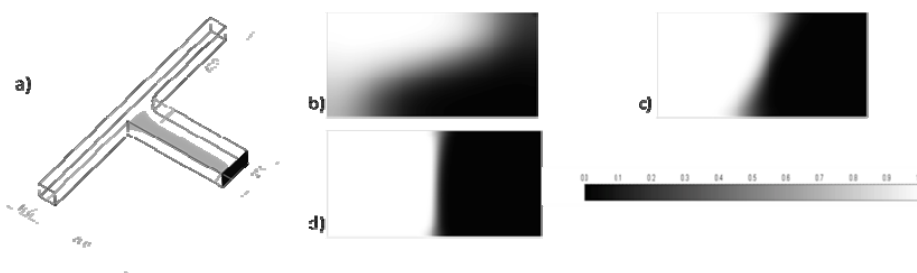


Figure 2: a) View of mixing geometry. All sizes are in  $\mu\text{m}$ . The outlet (darker region), is the selected region for mixing analyses. Mass fraction contour plots for W-E systems b) at  $Re=0.1$  c)  $Re=1$  and d)  $Re=10$ .

## 2.3 Degree of Mixing

As neither the volume flow rate nor the average concentration of the mixture are conserved as we move down the channel, we prefer to characterize the average properties of the mixture using the “cup mixing average”, or “bulk”, mass fraction (Middleman, 1998), that is the mass fraction that we would measure when we collect the efflux from the channel in a cup and mix the contents to yield a uniform composition,

$$\bar{\phi}_b = \frac{\dot{m}_A}{\dot{m}_{tot}} = \frac{\int_S \phi(\mathbf{r}) \rho(\mathbf{r}) u(\mathbf{r}) dy dz}{\int_S \rho(\mathbf{r}) u(\mathbf{r}) dy dz} = \frac{\sum_i^N \phi_i \rho_i u_i}{N \rho u}, \quad (6)$$

where  $\mathbf{r} = (x, y, z)$ ,  $N$  is the number of sampling points within the cross section of area  $S$ ,  $\bar{\phi}_b$  is the mass fraction of fluid A at point  $i$  in the cross section, with,

$$\dot{m}_{tot} = \bar{\rho} u S; \quad \bar{\rho}(x) = \frac{1}{S} \int_S \rho(\mathbf{r}) dy dz; \quad \bar{u}(x) = \frac{1}{S \bar{\rho}(x)} \int_S \rho(\mathbf{r}) u(\mathbf{r}) dy dz, \quad (7)$$

Accordingly, we use here a definition of mixing efficiency based on material fluxes, instead of concentrations, defining a volumetric flow variance as:

$$\sigma_b^2(x) = \frac{\int_S (\phi(\mathbf{r}) - \bar{\phi}_b)^2 \rho(\mathbf{r}) u(\mathbf{r}) dy dz}{\int_S \rho(\mathbf{r}) u(\mathbf{r}) dy dz} = \frac{1}{N \bar{\rho} u} \sum_{i=1}^N (\phi_i - \bar{\phi}_b)^2 \rho_i u_i \quad (8)$$

where  $\dot{m}_a = \bar{\phi}_b \bar{\rho} u$  is the prescribed mass flow rate of species A per unit area. Therefore, we can define the degree of mixing as  $\delta_m = 1 - \sigma_b / \sigma_{max}$ , where  $\sigma_{max} = \sqrt{\bar{\phi}_b(1 - \bar{\phi}_b)}$  is the maximum value of the variance, that is achieved when the two streams are completely segregated. This definition is similar, although not identical, to the one used by Glasgow and Aubry (2003) and Galletti et al. (2012). Obviously, we expect that  $\delta_m$  increases monotonically as we move down the mixing channel with  $x$ , tending asymptotically to 1 as the two fluids mix completely.

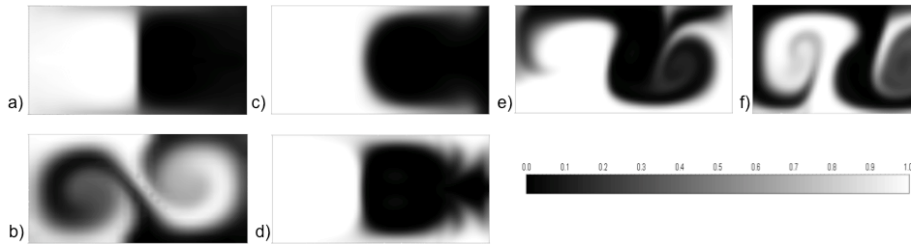


Figure 3: Mass fraction contour plots at the outlet cross-section a) for a W-W system at  $Re=100$  and b)  $Re=200$ ; for a W-E system c) at  $Re=100$ ; d) at  $Re=200$ ; e)  $Re=230$ ; f) at  $Re=300$ .

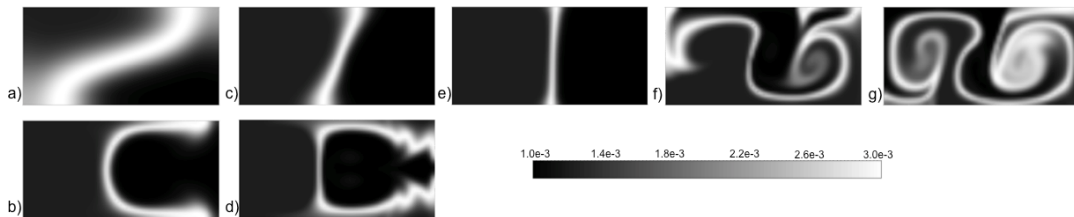


Figure 4: Viscosity contour plots for W-E systems when a)  $Re=0.1$ ; b)  $Re=100$ ; c)  $Re=1$ ; d)  $Re=200$ ; e)  $Re=10$ ; f)  $Re=230$ , and g)  $Re=300$ .

### 3. Results and discussion

The W-W case, where the two inlet fluids are both water, is compared with W-E case, when they consist of water and ethanol, imposing the same volumetric flow rates at the two inlets, i.e. using the same mean inlet velocity  $U$ , and assuming that inlet velocity profiles are fully developed. In the same way, the Reynolds number is defined using the mean inlet velocity,  $U$ , the hydraulic diameter  $d$  of the mixing channel and the kinematic viscosity of water. First of all, it should be noted that in the W-W case a vertical

interface region is stable and, in laminar flow with no mass diffusion, could remain unchanged as we move down the channel; on the other hand, in the W-E case this vertically segregated morphology is unstable and, in fact, as we move along the mixing channel, the water stream will progressively move down and occupy the lower part of the pipe, due to the water larger density, while the ethanol stream will move up. A simple dimensional analysis reveals that the interface will start deforming from its initial vertical position when the vertical, transversal velocity  $u$  will balance the viscous velocity,  $\mu/\rho d$ . Therefore, considering that  $U \cong uL/d$  from continuity, where  $U$  is the longitudinal velocity, we find:  $L/d \cong Re = U/(\mu/\rho d)$ . Since in our case  $L/d = 2.5$ , that explains why, at the exit of the mixing channel, when  $Re = 0.1$  the water stream has already occupied most of the lower part of the cross section, while when  $Re = 1$  this process is just starting to occur, and when  $Re = 10$  the W-E interface at the exit is still vertical (see the concentration contour plots in Figure 2). Then, at  $Re = 100$  the heavier liquid, i.e. water, tends to occupy the center of the cross section, where the velocity is larger due to its larger inertia, as was clearly shown by many investigators (Joseph et al., 1984). As a comparison, in Figure 3a we see that, at the same  $Re = 100$  but in the W-W case, the contour plot exhibits mirror symmetry, although a secondary flow occurs in the form of a double vortex pair, due to the instabilities induced by the centrifugal forces at the confluence. Finally, in the engulfment regime occurring beyond a certain critical Reynolds number, fluid elements reach the opposite side of the mixing channel, thus largely increasing the degree of mixing. Using a micro-mixer having a  $200 \times 100 \mu\text{m}$  mixing channel, Bothe et al. (2006) found that in the W-W case engulfment occurs at  $Re = 146$ ; also, Hoffmann et al. (2006) and Engler et al. (2004) indicated the engulfment to occur at  $135 < Re < 150$  and  $Re=147$ , respectively, for micro-mixers with the same aspect ratio. They all observed similar patterns even at larger Reynolds number; in fact, in Figure 3b, we show the engulfment contour plot at  $Re = 200$  for the W-W case. On the other hand, in the W-E case, the onset of engulfment is retarded, occurring at larger Reynolds numbers compared to the W-W case. In fact, as shown in Figure 3d, when  $Re = 200$  the concentration plot is quite similar to that at  $Re = 100$  (and therefore quite different than that of the W-W case at the same  $Re$ ). Then, as we progressively increase the inlet flow rates, at  $Re = 230$  we see the appearance of an engulfment flow (Figure 3e), with the concentration fields remaining basically unchanged as we move up to  $Re = 300$  (Figure 3f). This behavior is well explained in Figure 4, where the viscosity contour plots at the exit cross-section are represented for different  $Re$ . There, considering that the viscosity of a W-E mixture is quite larger than that of both components, we see that as  $Re$  increases from 0.1 to 10 the width of the mixing region narrows; then, as  $Re$  increases to 100 and 200, we see the more viscous fluid tending to occupy the center of the cross section until, at  $Re = 230$ , engulfment appears and the extent of the mixing region increases. From these viscosity plots we can conclude that when we try to mix water and ethanol, vortex formation is hampered by the more viscous mixture that emerges from the contact between the two streams at the confluence, thus retarding the onset of engulfment. Our results are summarized in Figure 5, where the degree of mixing is plotted as a function of the Reynolds number for both W-W and W-E cases. As  $Re$  varies between 0.1 and 1 the degree of mixing is consistently higher in the W-E than in the W-W case, due to the larger residence time resulting from slower fluid velocity, above all in the interfacial region, which results to be almost horizontal. Then, for  $1 < Re < 10$ , the degree of mixing is about the same in the two cases until, at the onset of the engulfment flow, the degree of mixing greatly increases; that happens at  $Re \cong 140$  in the W-W case and at  $Re \cong 230$  in the W-E case. It should also be noted that, if we assume viscosity to be a linear function of the mass fraction, which is the default choice of most CFD programs, in the  $1 < Re < 10$  range we would find a 10-20% smaller degree of mixing.

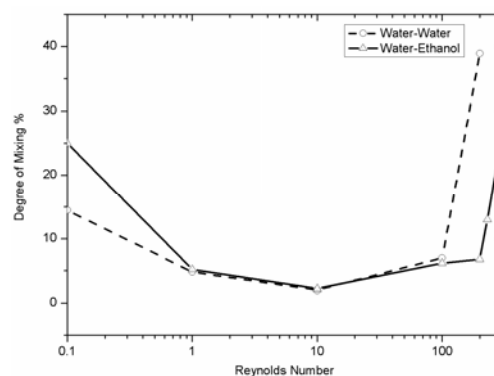


Figure 5: Degree of mixing as a function of the Reynolds number for W-W and W-E systems.

#### 4. Conclusions

We showed that, at smaller Reynolds numbers,  $Re < 100$ , mixing is controlled by transverse diffusion, and therefore by the residence time of each fluids. Accordingly, as ethanol is slightly more viscous than water and therefore it flows slower, the degree of mixing in the W-E case is slightly larger than that of the W-W case. On the other hand, at larger Reynolds numbers, mixing water and ethanol may take considerably longer, as the onset of engulfment is retarded and occurs at larger Reynolds numbers, namely increasing  $Re \cong 140$  in the W-W case to at  $Re \cong 230$  in the W-E case. In fact, at the confluence between the water and the ethanol streams, a W-E mixture forms that is two to three times more viscous than water alone; this viscous layer separating the two streams will hamper any vortex formation, thus opposing mixing.

#### Acknowledgment

This work was supported in part by the Italian Ministry of Education and Research (MIUR), Grant PRIN, no.2009-3JPM5Z.

#### References

- Ansari, M.A., Kim, K.Y., Kim, S.M., 2010. Numerical study of the effect on mixing of the position of fluid stream interfaces in a rectangular microchannel. *Microsystem Technologies* 16, 1757–1763.
- Bothe, D., Stemich, C., Warnecke, H.J., 2006. Fluid mixing in a T-shaped micro-mixer. *Chemical Engineering Science* 61, 2950–2958.
- Bothe, D., Stemich, C., Warnecke, H.J., 2008. Computation of scales and quality of mixing in a T-shaped microreactor. *Computers & Chemical Engineering* 32, 108–114.
- Chung, C.K., Shih, T.R., 2008. Effect of geometry on fluid mixing of the rhombic micromixers, *Microfluid Nanofluid* 4, 419–425.
- Dizechi, M., Marschall, E. 1982. Viscosity of some binary and ternary liquid mixtures. *Journal of Chemical Engineering Data* 27, 358-363.
- Engler, M., Kockmann, N., Kiefer, T., Woias, P., 2004. Numerical and experimental investigations on liquid mixing in static micromixers. *Chemical Engineering Journal* 101, 315–322.
- Galletti, C., Roudgar, M., Brunazzi, E., Mauri, R., 2012. Effect of inlet conditions on the engulfment pattern in a T-shaped micro-mixer. *Chemical Engineering Journal* 185-186, 300-313.
- Glasgow, I., Aubry, N., 2003. Enhancement of microfluidic mixing using time pulsing. *Lab on a Chip* 3, 114-120.
- Happel, J., Brenner, H., 1973. *Low Reynolds Number Hydrodynamics*. Noordhoff, Amsterdam.
- Hessel, V., Lowe, H., Schonfeld, F., 2005. Micromixers - a review on passive and active mixing principles. *Chemical Engineering Science* 60, 2479– 2501.
- Hoffmann, M., Schluter, M., Rabiger, N., 2006. Experimental investigation of liquid-liquid mixing in T-shaped micro-mixers using  $\mu$ -LIF and  $\mu$ -PIV. *Chemical Engineering Science* 61, 2968–2976.
- Hussong, J., Lindken, R., Pourquie, M., Westerweel, J., 2009. Numerical study on the flow physics of a T-shaped micro mixer, in: Ellero, M., et al. (Eds.), *IUTAM Symposium on Advances in Micro- and Nano-fluidics*. Springer, Heidelberg, pp. 191–205.
- Joseph, D.D., Nguyen, K., Beavers, G.S., 1984. Non-uniqueness and stability of the configuration of flow of immiscible fluids with different viscosities. *Journal of Fluid Mechanics* 141, 319-345.
- Kern, D.Q., 1965. *Process Heat Transfer*. McGraw-Hill, New York, p. 161.
- Lin, Y., Yu, X., Wang, Z., Tu, S.T., Wang, Z., 2011. Design and evaluation of an easily fabricated micromixer with three-dimensional periodic perturbation. *Chemical Engineering Journal* 171, 291–300.
- Middleman, S., 1998. *An Introduction to Mass and Heat Transfer*. Wiley, New York, USA, 217-218.
- Nguyen, N.T., Wu, Z.G., 2005. Micromixers - a review. *Journal of Micromechanics and Microengineering* 15, 1–16.
- Perry, R.H., Green, D.W., 1997. *Perry's Chemical Engineers' Handbook*, 7th ed. McGraw Hill, New York, Table 2-111.
- Roudgar, M., Brunazzi, E., Galletti, C., Mauri, R., 2012. Numerical study of split T-micromixers, *Chemical Engineering & Technology* 35, 1291–1299.
- Vural-Gürsel, I., Wang, Q., Noël, T., Hessel, V., 2012. Process-design intensification – direct synthesis of adipic acid in flow, *Chemical Engineering Transaction*, 29, 565-571.